AIAA JOURNAL
Vol. 38, No. 10, October 2000

Experiments on Mach-Wave Interactions in a Compressible Shear Layer

Michael J. Doty* and Dennis K. McLaughlin†
Pennsylvania State University, University Park, Pennsylvania 16802

A potential technique for improving the growth rate of compressible shear layers is studied, in which a wavy-wall geometry is configured in a confined supersonic shear-layer facility that generates Mach waves in the flowfield. The major objective of this work is to evaluate a numerical model that predicts the growth properties of a three-way resonant interaction of these spatial Mach waves with duct acoustic waves and Kelvin–Helmholtz waves excited artificially or naturally within the shear layer. Measurements show that a tuned pure tone excitation of Kelvin–Helmholtz waves couples with the wavy-wall-induced disturbances and duct acoustic waves to produce local shear-layer growth rates that are approximately 50% higher than the natural, smooth-walled baseline case. The conditions for optimum growth rates are in general concurrence with numerical predictions. In this study the flow physics of a compressible shear layer in a wavy-wall environment was investigated with mean and fluctuating flowfield measurements, as well as schlieren visualizations.

Nomenclature

a	= speed of sound
C	= C neutral acoustic wave
D	= D neutral acoustic wave
D_{03}	= third transverse mode of D neutral acoustic wave (zeroth spanwise mode, two-dimensional)
f	= excitation frequency
f_c	= characteristic frequency
H	= channel height
KH	= Kelvin–Helmholtz instability wave
k	= wave number
M	= Mach number
$M_{c\,(\text{theoretical})}$	= theoretical convective Mach number
m'	= rms mass-velocity fluctuation level (normalized by local mean mass velocity value)
P_0	= stagnation pressure
Re	= Reynolds number
Sr	= Strouhal number
T_0	= stagnation temperature
U	= streamwise velocity component
x	= streamwise coordinate
y	= transverse coordinate
ΔU	= streamwise velocity difference, $U_1 - U_2$
δ_ω	= shear-layer vorticity thickness
δ'	= compressible shear-layer growth rate
δ'_0	= incompressible shear-layer growth rate
λ	= wavelength
ρ	= density
σ_r	= resonant growth rate
ω	= radian frequency

Subscripts

C	= C neutral acoustic mode
D	= D neutral acoustic mode
i	= ith Fourier component
KH	= Kelvin–Helmholtz instability
M	= Mach wave
1	= high-speed stream
2	= low-speed stream

Presented as Paper 99-2105 at the AIAA/ASME/SAE/ASEE Joint Propulsion Conference, Los Angeles, CA, 20–24 June 1999; received 20 July 1999; revision received 17 March 2000; accepted for publication 27 March 2000.

*Graduate Student, Department of Aerospace Engineering. Member AIAA.
†Professor and Head of Aerospace Engineering, Department of Aerospace Engineering. Associate Fellow AIAA.

Introduction

REUSABLE launch vehicles, advanced hypersonic missiles, and future supersonic transport aircraft all require advances in high-speed propulsion systems, which, in turn, involve a greater understanding of compressible mixing layers. One specific area in which compressible mixing layers play a fundamental role is in the development of scramjet propulsion systems. To accomplish thorough combustion within the length of the combustor section where air and fuel streams form a compressible mixing layer, successful methods of mixing enhancement with minimal performance penalty must be developed. It is the study of compressible mixing layers and mixing enhancement, as it applies to scramjet design applications, that motivates this work.

The flow physics governing incompressible mixing layers is now well understood with the renowned work of Brown and Roshko[1] and many others.[2–6] However, the level of understanding decreases with compressibility. The decrease in mixing layer growth rate with increasing Mach number is well documented.[7–9] Nonetheless, the exact mechanisms involved in the decreased compressible mixing layer growth rate are still open to debate. Without a complete understanding of this phenomenon, the development of mixing enhancement techniques has had marginal success.[10–13] The current work experimentally examines a shear-layer growth rate enhancement technique using Mach-wave interactions. Tam and Hu[14,15] performed computational studies demonstrating that a Mach-wave pattern generated from a wavy-wall geometry could force a resonant interaction with two additional families of waves in a ducted shear layer. Gilreath et al.[16] performed initial wavy-wall experiments and found no significant growth rate enhancement. Lee[17] proposed a modified version of the Tam and Hu[14,15] theory focused on involving the Kelvin–Helmholtz instabilities in the resonant interaction, and Martens and McLaughlin[18] performed limited experiments comparing to the numerical results of Lee[17] with some success. However, the computational efforts of Lee were not completed until after Martens's experiments. Thus, this work extends these comparisons with the benefit of having the computational results a priori, allowing more direct comparisons. The major objective of the present study was to examine experimentally the three-way resonant interaction in a supersonic shear layer predicted by Lee[17] to produce significantly increased growth rates.

An important part of the study involves the characterization of the basic compressible flow physics within a wavy-wall environment. Pressure and hot-wire measurements are compared to qualitative schlieren flow visualization images. Experiments investigate the

approximate location of maximum fluctuation levels within the shear layer and compare mass-velocity fluctuation levels to shear-layer vorticity thickness growth.

Before proceeding further, a brief point concerning semantics is necessary. Up to this point, the terms mixing layer and shear layer have both been used to describe the region of fluid existing between two streams. A mixing layer is a type of free shear layer; however, one should take note that a true mixing layer requires turbulent flow. A laminar layer exhibits shear between the fluid streams but no real mixing because the fluids each retain their organized streamlines. The low-Reynolds-number facility used in the present study produces a laminar shear layer at the splitter plate. Thus, the experiments in this work focus on shear-layer growth rate as a measure of merit that is assumed indicative of, but not analogous to, mixing enhancement.

Experimental Facility

General Description

The supersonic shear-layer facility uses a combination of compressed air and high vacuum to generate supersonic flows in two streams. A schematic of the facility is shown in Fig. 1. Before an experiment, a vacuum pump evacuates the air in three pressure recovery tanks, as well as the facility shell, until the pressures are less than one torr (0.13 kPa). The majority of the driving pressure difference is created from this high vacuum. The remainder of the pressure difference is generated by the delivery of compressed air that has been dried and filtered. The treated air of approximately 3 atm (304 kPa) is divided into a high- and low-speed stream as it passes through pressure control valves.

Each stream is conditioned in the settling chamber before accelerating through two supersonic nozzles. The two streams meet again at the tip of the splitter plate, and a shear layer is generated in the test section. The splitter plate tip angle is approximately 4 deg with a final thickness of 0.03 cm. The test section measures 5 cm high by 12.5 cm wide by 75 cm long and is equipped with a traverse system and optical sidewalls for visualization. The high-speed stream is located below the low-speed stream.

The tip of the splitter plate is equipped with a glow discharge device used to excite the flow. This device uses a fluctuating voltage input to create a high-temperature glow between a copper electrode strip and the aluminum splitter plate. Figure 2 shows the effects of the glow excitation on the shear-layer flow. Downstream of the test section, the two streams are separated once more by a split stream diffuser as each stream flows into its own pressure recovery tank(s). The facility is described in greater detail in Refs. 19 and 20.

Flow Parameters

The Mach-number range of the supersonic shear-layer facility is Mach 2–4 for the high-speed stream and sonic to $M = 2.5$ for the low-speed stream. The simplified theoretical convective Mach number developed by Papamoschou and Roshko[9] is

$$M_{c\,(\text{theoretical})} = (U_1 - U_2)/(a_1 + a_2) \tag{1}$$

Using Eq. (1), the convective Mach-number upper limit of the facility is $M_{c\,(\text{theoretical})} \approx 0.74$.

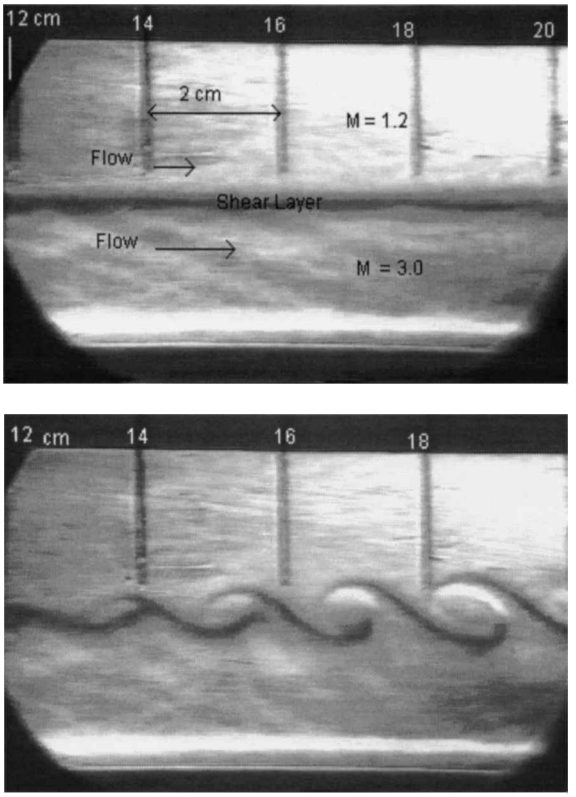

Fig. 2 Schlieren images of flowfield beginning 12 cm downstream from the splitter plate for the a) natural shear layer and b) shear layer with 30-kHz excitation.

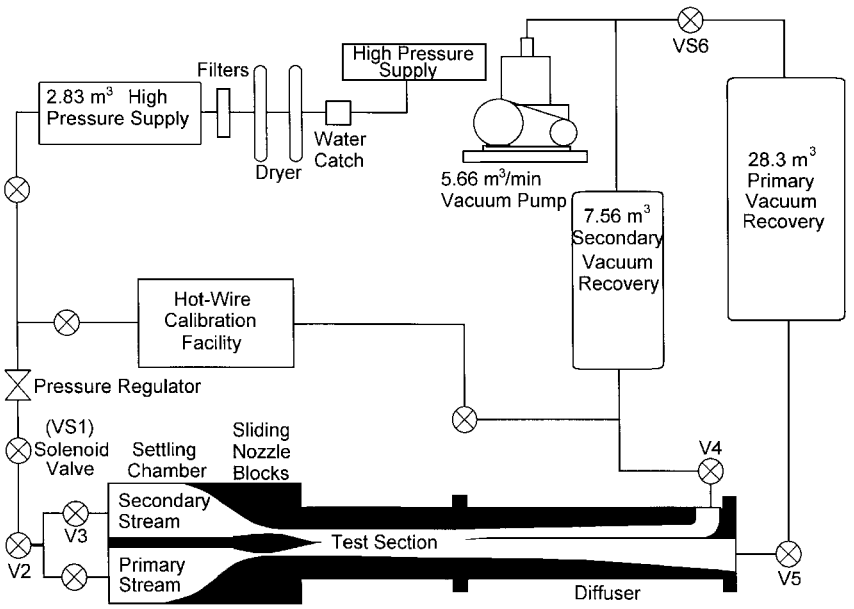

Fig. 1 Schematic of supersonic shear-layer facility.

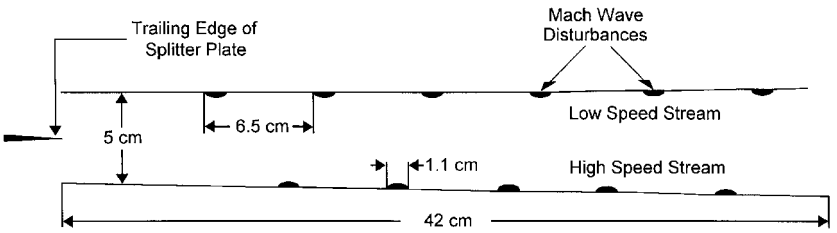

Fig. 3 Schematic of wavy-wall geometry within test section.

The Reynolds-number range for this facility (2×10^4 to 7×10^4 cm^{-1}, based on high-speed stream flow conditions) is approximately an order of magnitude lower than most similar facilities[9,16] because of the high vacuum design. This low-Reynolds-number regime restricts direct comparisons to realistic scramjet systems. Furthermore, the low-density environment hampers the resolution of the schlieren images. However, the low-Reynolds-number operation does facilitate the examination of the three-way resonant interaction described by Lee[17] in a way not possible in a conventional high-Reynolds-number facility. Specifically, the low-Reynolds-number operation, involving low-to-moderate-density flow, facilitates the operation of the glow discharge excitation and the use of conventional hot wires within the flow.

Mach-Wave Interaction Technique

Theoretical Overview

The Mach-wave interaction technique involves creating a resonant interaction among various instability waves and a standing Mach-wave pattern induced from a wavy wall. Tam and Hu[14,15] originally developed a theory describing a resonant interaction among periodic spatial Mach waves, duct acoustic modes, and a newly discovered class of shear-layer instability waves they call supersonic instabilities.

Lee[17] performed a computational study similar to that of Tam and Hu[15] but with a focus on Kelvin–Helmholtz instabilities. Lee[17] was motivated by the work of Gathmann et al.[21] whose simulations did not find significant shear-layer growth rate enhancement with the supersonic instabilities and the duct acoustic modes. Gathmann et al.[21] did find, however, that the oblique (three-dimensional) Kelvin–Helmholtz instabilities can be responsible for increased growth rates of the supersonically convecting shear layer.

Lee[17] focused on two-dimensional Kelvin–Helmholtz instabilities in a subsonically convecting shear layer as an initial study on the effectiveness of the Mach-wave interaction growth rate enhancement technique. As with the Tam and Hu[15] theory, the duct acoustic modes are important in the resonant interaction. Lee[17] found a resonance condition given by

$$k_{M_{(i)}} = k_{\mathrm{KH}} - k_D \quad \text{or} \quad k_{M_{(i)}} = k_C - k_{\mathrm{KH}}, \qquad i = 1, 2, 3, \ldots \tag{2}$$

Using the relationship between wave number and wavelength

$$k = 2\pi/\lambda \tag{3}$$

Equation (2) can be expressed as

$$\lambda_{M_{(i)}} = \frac{\lambda_{\mathrm{KH}}\lambda_D}{\lambda_D - \lambda_{\mathrm{KH}}} \quad \text{or} \quad \lambda_{M_{(i)}} = \frac{\lambda_C\lambda_{\mathrm{KH}}}{\lambda_{\mathrm{KH}} - \lambda_C}, \qquad i = 1, 2, 3, \ldots \tag{4}$$

The results obtained for the growth rates in this computational analysis were approximately three times larger than those of the natural Kelvin–Helmholtz instability waves in certain cases.

As already mentioned, initial wavy-wall, confined supersonic shear-layer experiments were performed by Gilreath et al.[16] and later by Gustafson et al.[22] Rather than matching the resonance conditions just discussed, they matched the wavy-wall wavelength to the most unstable Kelvin–Helmholtz instability and found little evidence of enhanced shear-layer growth rate.

On the other hand, Martens and McLaughlin[18] performed similar experiments (in the present facility) matching the wavy-wall wavelength to the resonance condition developed by Lee[17] as shown in Eq. (4). With this approach they were able to report local growth rate increases by as much as 50% with no glow excitation, to 100% with 20-kHz glow excitation. (Note that the relationship between dimensional frequency and the shear-layer characteristic frequency is discussed later in this paper.) At these same experimental conditions Lee's[17] numerical analysis shows an interaction among the Kelvin–Helmholtz instabilities, the D_{03} acoustic mode, and spatial Mach waves to produce significantly increased shear-layer growth rates. It is this resonant interaction that is the focus of this experimental study.

Wavy-Wall Setup

The current work extends Martens and McLaughlin's experiments[18] by measuring shear-layer thickness at more streamwise locations and excitation conditions, as well as taking complimentary hot-wire measurements and schlieren observations. The wavy-wall geometry within the test section is depicted in Fig. 3. The amplitude and wavelength were chosen to be the same as the most promising case presented by Martens and McLaughlin.[18]

The hemispherical disturbances have an amplitude of 0.15 cm and a width of 1.1 cm. The disturbance amplitude is small enough to allow attached boundary layers through the measurement area, yet large enough to be machined relatively easily. The disturbances are held in place by two small machine screws extending through slots in the test section floor and ceiling.

The wavelength of the disturbances is 6.5 cm and is determined by satisfying the no-reflection boundary condition described in Martens.[20] The wavelength and length of the measurement region dictate the use of six disturbances on the low-speed side (top wall) and five disturbances on the high-speed side (bottom wall) as seen in Fig. 3. The number of disturbances is later varied when performing a study of growth rate enhancement vs total pressure loss.

Lee's[17] numerical analysis is used in the experiments to investigate an optimum resonance condition, not by varying the Mach-wave wavelength, but rather by varying the Kelvin–Helmholtz instability wavelength in Eq. (4). This is accomplished by exciting specific spectral components of the Kelvin–Helmholtz instability through the use of the glow discharge excitation system. The effectiveness of this method is verified in Ref. 19 using schlieren visualizations, such as that of Fig. 2b, to determine wavelength and convection velocity.

Experimental Results

Mean Flowfield

The mean flowfield data are collected throughout the shear layer using a 10-port pitot probe with a spatial resolution between ports of approximately 1.6 mm. The probe was located in a spanwise location near the center of the test section and remained in this spanwise location for the duration of the experiments. The experimental conditions for both the mean and fluctuating flowfield measurements are presented in Table 1. Total temperature measurements are not performed within the facility for the current experiments. Prior experiments have shown that the stagnation temperature in the upstream settling chamber is within experimental uncertainty (±3%) of room temperature for this facility. The last parameter in Table 1 is a measure of the characteristic frequency of the facility:

$$f_c = U_1/H \tag{5}$$

One set of conditions, corresponding to that of Martens and McLaughlin,[18] was chosen for the majority of experiments for valid

Table 1 Experimental conditions

Parameter	Value
M_1	3.0
M_2	1.2
T_0,[a] K	293
$M_{c\,(theoretical)}$	0.5
P_{01}, kPa	42.7; 66.7
Re, cm^{-1}	3.3×10^4[b]; 5.15×10^4
f_c, Hz	12,300

[a]Assumed based on room temperature measurement.
[b]This value was incorrectly reported as 4×10^4 cm^{-1} in Martens and McLaughlin.[18]

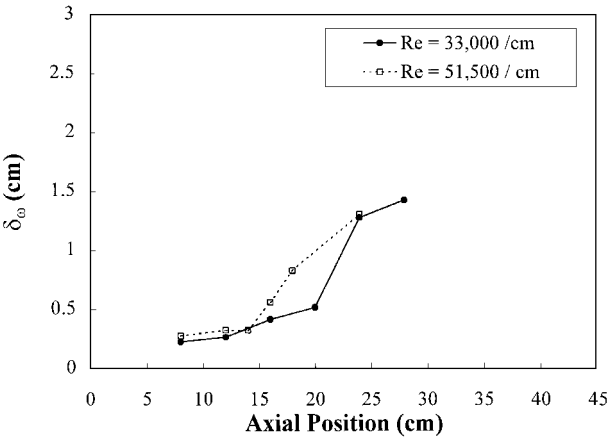

Fig. 4 Reynolds-number effects on shear-layer vorticity thickness.

comparisons to be made. In addition, a second condition of higher total pressure was chosen to investigate briefly the effects of a higher Reynolds number.

The shear-layer thickness is measured in terms of a vorticity thickness δ_ω, defined as

$$\delta_\omega = \frac{\delta U}{(\partial U/\partial y)_{\max}} \tag{6}$$

The determination of δ_ω is accomplished through a simple geometric technique applied to the shear-layer velocity profile plot as detailed in Ref. 18. Although a straightforward technique, the determination of the vorticity thickness is, however, limited in its accuracy. The uncertainty associated with the measurements is approximately 10% at an axial location midway down the test section. This uncertainty is caused primarily by the arbitrary nature of the line-fitting geometric technique to determine δ_ω. Thus, hot-wire and schlieren measurements are presented to characterize the shear layer more completely.

Before investigation of the growth rate enhancement mechanism, the effect of Reynolds number on the behavior of the shear layer was analyzed. For the unexcited shear layer in a smooth-wall environment (no wavy-wall disturbances on the test section floor or ceiling), two different Reynolds numbers were tested. Figure 4 shows the vorticity thickness for each case at various downstream locations. It appears that the Reynolds number has little effect on the overall growth of the shear layer, but rather affects only the transition point. Reynolds-number-independent shear-layer growth is expected based on previous works such as Browand and Troutt's[23] incompressible study reporting that the large-scale structures largely responsible for growth were present in both the laminar and turbulent shear layers and were mostly independent of Reynolds number.

The issue of transition is important in this low-Reynolds-number facility. Regardless of Reynolds number, all shear-layer experiments in this study initiate from laminar boundary layers along the top and bottom of the splitter plate. The wake of the splitter plate is evident in the laminar shear-layer profile up to 12 cm, but disappears further downstream at 16 cm (see Ref. 19 for details). Furthermore, the initial laminar shear-layer undergoes transition to a turbulent shear layer at some point further downstream after the disappearance of the wake component. As Fig. 4 demonstrates, this transition location

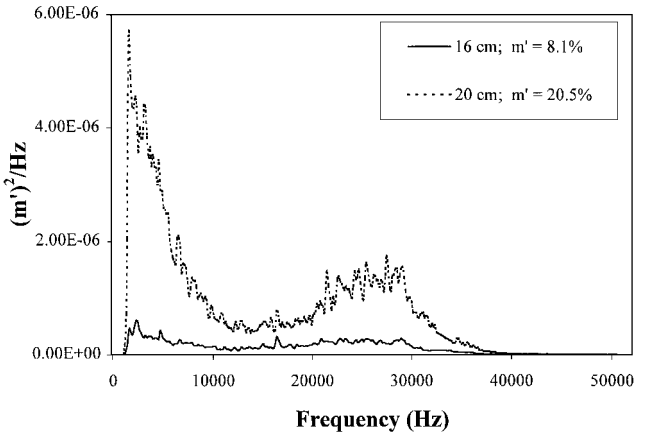

Fig. 5 Hot-wire spectra ($Re = 3.3 \times 10^4$ cm^{-1}) showing increased mass-velocity fluctuations indicating transition to turbulence from 16 to 20 cm downstream.

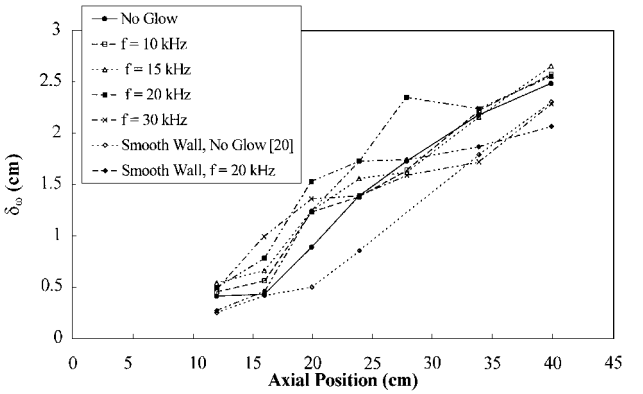

Fig. 6 Vorticity thickness vs streamwise distance with the wavy-wall geometry for five cases of various excitation and with two smooth-wall cases for comparison.

is Reynolds number dependent. The $Re = 3.3 \times 10^4$ cm^{-1} case transitions in a region from approximately 20–24 cm downstream of the splitter plate. Evidence of this transition near 20 cm can also be seen in hot-wire spectral plots shown in Fig. 5 in which a dramatic increase in mass-velocity fluctuation level and broadband activity is seen in going from 16 to 20 cm downstream. So as not to confuse enhanced shear-layer growth with transition to turbulence, it is important to note the location of this transition region in all experiments.

The majority of the mean flow measurements taken with the wavy-wall disturbances in place can be summarized in Fig. 6. Shear-layer vorticity thickness is plotted vs streamwise location for various excitation frequencies. The measurements are taken at $Re = 3.3 \times 10^4$ cm^{-1}, as are the remainder of the measurements described in this work, unless otherwise noted. Shear-layer thicknesses are measured from 12 to 40 cm downstream of the splitter plate. These distances were dictated by the splitter plate wake region that is prevalent up to 12 cm and the merging of the shear layer and boundary layers, which occurs near 40 cm downstream. Many of the differences in data in Fig. 6 are within the uncertainty of the experiments (10%); therefore, interpretation focuses on the noticeable trends, which also compare with the hot-wire results that follow.

Figure 6 shows that the 20-kHz excitation case appears to have the largest growth of any case along the majority of the measurement region. The 30-kHz case shows the quickest initial growth near 15 cm but then decreases considerably, whereas the 10- and 15-kHz cases exhibit increased shear-layer thicknesses over the unexcited case at further upstream locations. In addition, two smooth-wall cases are included for comparison—the baseline condition of smooth walls with no excitation taken from Martens[20] and the smooth-wall, 20-kHz excitation case. All wavy-wall cases show improved growth over the baseline smooth-wall unexcited case, whereas the smooth-wall, 20-kHz excitation case shows comparable growth in the

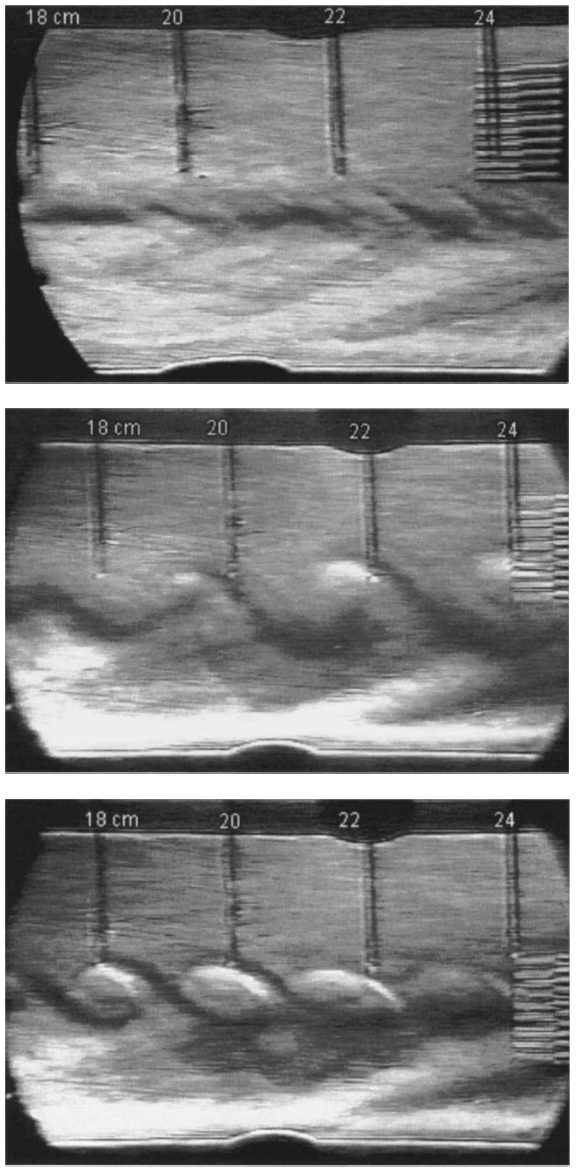

Fig. 7 Schlieren images of the shear layer approximately 18–24 cm downstream with wavy-wall geometry in place for excitation cases of a) no excitation, b) 20 kHz, and c) 30 kHz.

upstream region, but begins to level off farther downstream. This is consistent with the premise that some resonant interaction is taking place involving the wavy-wall disturbances.

Figure 7 shows corresponding schlieren flow visualizations of select cases. The large-scale structures seem to be limited in size at the 30-kHz excitation, thus resulting in a thinner shear layer.

As the shear layer thickens, its dominant length scale increases, and the dominant frequency decreases. A decrease in dominant shear-layer frequency with downstream distance results in the eventual ineffectiveness of higher excitation frequencies, a result also found by Lee.[17] In fact, such excitations can result in destructive interference, and excited shear layers can actually show less growth than their unexcited counterparts, as evidenced in Fig. 6 for the 30-kHz case. It is also thought that the shear-layer growth is impeded by the wall boundary layers at further downstream locations where a plateau in growth rate becomes apparent.

It is important to remember that the mechanisms for enhancement in these experiments are actually more complex than a simple forcing at the dominant shear-layer frequency. With the standing Mach-wave pattern present, a three-wave interaction is theoretically taking place in which the Mach waves and neutral acoustic waves (class C or D following the definition of Lee[17]) interact to drive the Kelvin–Helmholtz instability to resonance. Although it is difficult to prove experimentally that specific wave modes are involved in

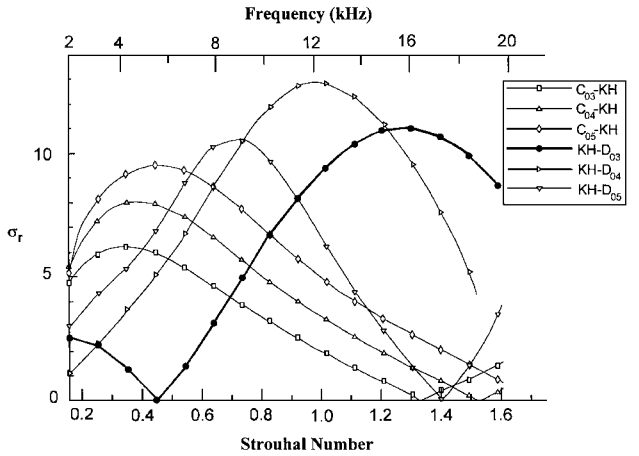

Fig. 8 Numerical results showing resonant growth rates σ_r for C and D: KH interactions at 12 cm downstream, from Lee.[17]

resonant interactions while others are not, an attempt is made to compare to the trends of Lee's[17] numerical results.

Figure 8 shows Lee's[17] numerical results of resonant growth rates for different C and D wave interactions with the Kelvin–Helmholtz instability (KH) waves at 12 cm downstream. Using the following definition of Strouhal number

$$Sr = fH/U_1 = f/f_c \tag{7}$$

makes use of the previously defined characteristic frequency f_c from Eq. (5). (Note that Lee's[17] definition, which has not been completely adopted in this work, defines Strouhal number based upon circular frequency in radians per second as well as the channel height H.) Figure 8 shows Lee's predicted resonant growth rate σ_r as a function of the Strouhal number defined in Eq. (7) (and the corresponding dimensional frequency corresponding to the current experiments). H was used in place of δ_ω as the length scale because vorticity thickness information was not part of Lee's[17] computational model.

Based on Lee's[17] previous analysis, the 6.5-cm wavy-wall wavelength spacing allows a resonant interaction between the KH waves and the D_{03} mode (shown in bold). Furthermore, Fig. 8 shows the resonant interaction to occur most notably at two frequencies $Sr = 0.19$ and 1.24, the latter corresponding to a dimensional frequency of 15.3 kHz. These resonant interaction points are spectral locations where theoretical prediction yields a broad peak in resonant growth rate, as first defined by Tam and Hu.[15] The experimental results of Fig. 6 show increased growth primarily at 20 kHz ($Sr = 1.63$) and 15 kHz ($Sr = 1.22$), and thus compare reasonably well with the numerical results. The tendency of the experiments to show more growth at 20 kHz than at 15 kHz, as expected from Lee's[17] results, is attributed to the fact that the numerical results are computed for the 12-cm downstream location specifically and cannot be accurately generalized over the entire range of measurements. Rates of shear-layer growth can also be computed from the data in Fig. 6. The growth rates are calculated from the region of noticeable growth from 16 to 28 cm downstream with a simple linear fit, consistent with Martens and McLaughlin.[18] Whereas 16–28 cm is a localized region that most likely incorporates transition, the reason for choosing this region to study the growth rate is twofold: it is the region downstream of the splitter plate wake, and it is the region upstream of the location where the leveling off of growth rate occurs. This plateau region, as already mentioned, is thought to be caused by the confinement of the shear layer by the influence of the top and bottom test section walls.

In an effort to compare these growth rates with other researchers, the incompressible shear-layer growth rate of the same density and velocity profiles is typically computed and used as a normalization parameter following Papamoschou and Roshko's[9] formulation. Figure 9 shows the results of various researchers[9,20,24,25] as well as the present data in terms of normalized growth rate vs convective Mach number. These growth rates are probably slightly overestimated compared to data outside of the Pennsylvania State University

Table 2 Wavy-wall disturbance optimization at 28 cm, 20-kHz excitation

Disturbances (number on top wall/number on bottom wall)	δ_ω, cm	P_{01} loss (from 12 up to 28 cm), %
Full set (6/5)	2.35	15.3
High speed, bottom wall only (0/5)	2.1	10.3
First two on bottom wall (0/2)	1.93	10.6
Smooth wall (0/0)	1.74	11.9

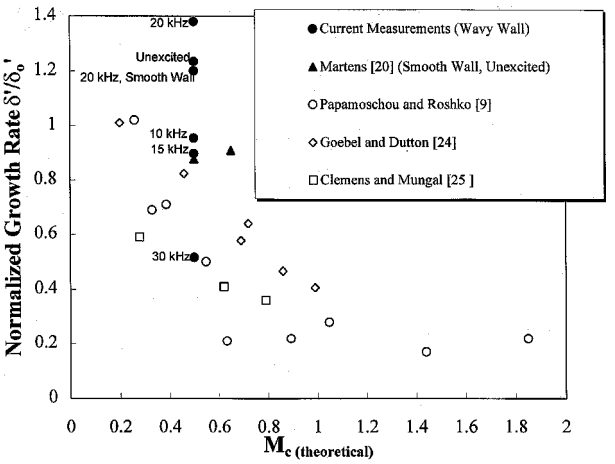

Fig. 9 Various experimentalists' results of compressible shear-layer growth rate normalized by the associated incompressible value, plotted vs $M_{c\,(theoretical)}$.

facility because of the existence of the transition region already mentioned.

The present experiments using the Mach-wave resonant interaction show increased growth rates for the unexcited and 20-kHz cases, whereas the other excited cases fall within the range of previous data. The local growth rate before normalization for the 20-kHz case was approximately 0.123 cm/cm, representing a 50% increase from the smooth-wall unexcited case (0.08 cm/cm) of Martens.[20] However, Martens and McLaughlin[18] found slightly higher levels of increase (~100%) in their initial wavy-wall experiments.

A final set of mean flow experiments focuses on the performance penalty of decreased momentum flux levels caused by total pressure losses associated with the wavy-wall disturbances. As the number of disturbances decreases, the total pressure loss decreases. However, the shear-layer growth also decreases with fewer disturbances, as also found by Gustafson et al.[22] The shear-layer (vorticity) thickness and high-speed stream total pressure loss are calculated from the pitot pressure measurements for various configurations. The total pressure losses are computed by taking the difference between the average high-speed freestream total pressure at the location of interest (28 cm) and the furthest measured upstream location (12 cm). Four cases are shown in Table 2, all of which are conducted at the conditions of highest observed shear-layer growth—a 20-kHz excitation with measurements made at 28 cm downstream. The rationale for the configurations tested is that the high-speed side generates stronger Mach waves; thus, those disturbances should be left in place, or at least a few of them, in order to initiate the Mach-wave pattern.

An unexpected result is the slight increase in total pressure loss for the last two cases. The inaccurate adjustment of the test section walls to account for less blockage with each successive configuration could be the source of these results. Without specific performance goals it is difficult to judge what shear-layer thicknesses and pressure losses are acceptable in such a trade study. Thus, the full set of disturbances (6 on top wall, 5 on bottom wall, each at 6.5 cm spacing) was used for consistency throughout the experiments.

When the entire measured pressure profile of roughly 20 data points is considered in the loss calculations, as shown in Fig. 10, and a mass-weighted integration of the profile is performed in terms of ρU^2 values, slightly lower pressure losses result. For the full disturbance case this results in approximately a 14.4% loss in integrated total pressure between 12 and 28 cm downstream.

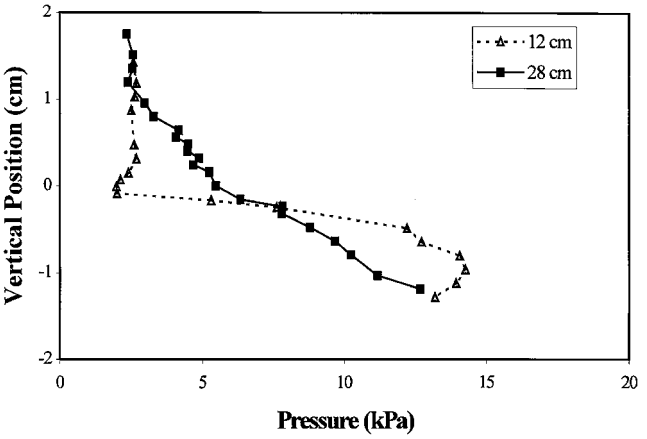

Fig. 10 Total pressure profiles (wavy-wall configuration, 20-kHz excitation) demonstrating the changing pressure profile with downstream distance.

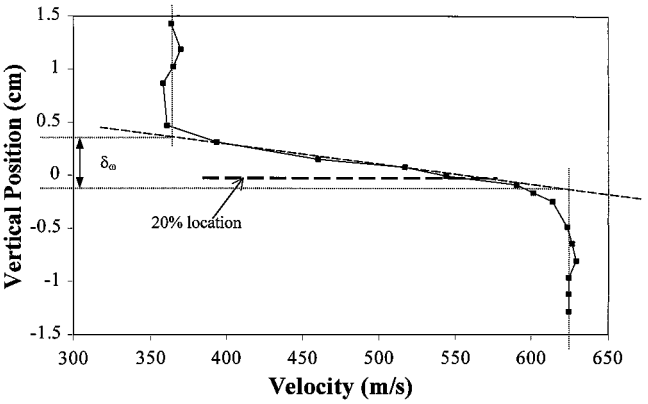

Fig. 11 Velocity profile 16 cm downstream (unexcited, smooth-wall case, $Re = 5.15 \times 10^4$ cm^{-1}) showing hot-wire probe location at 20% of local shear-layer thickness inside high-speed boundary.

Fluctuating Flowfield

Hot-wire measurements in compressible flow require special considerations. The fluctuation levels are reported as mass-velocity fluctuations as a result of the added variable of density. A single hot wire was used to collect information on the spectral content and relative mass-velocity fluctuation levels within the shear layer. Furthermore, the relationship between fluctuation level and shear-layer growth helps solidify understanding of the complex energy exchanges involved in turbulent flow.

To determine the maximum fluctuation level of the shear layer at a particular downstream distance, one would typically take numerous measurements at fine spatial increments, requiring large amounts of time and data storage capability. An alternative approach is sought in which one measurement is taken at a location estimated to be the location of the approximate maximum fluctuation level within the shear layer.

Because large-scale structures dominate the shear layer, it seems reasonable to expect maximum fluctuations to occur in a consistent region of the shear layer relative to its local thickness—for instance, at some percentage of the local shear-layer thickness within the shear-layer boundary. The shear-layer boundary is defined as the point at which deviations from the freestream velocity are first seen, as dictated by the geometric process of determining δ_ω already mentioned. Preliminary experiments and previous results from Martens[20] indicate that a vertical position approximately 20% of the local shear-layer thickness into the high-speed side of the shear layer exhibits the highest mass-velocity fluctuation levels. A quantitative illustration of the 20% location relative to a velocity profile is shown in Fig. 11. A more detailed examination of this 20% approximation is given in Ref. 19, in which hot-wire measurements at various vertical positions indicate that maximum fluctuation levels consistently occur at or near the 20% location. Demetriades and

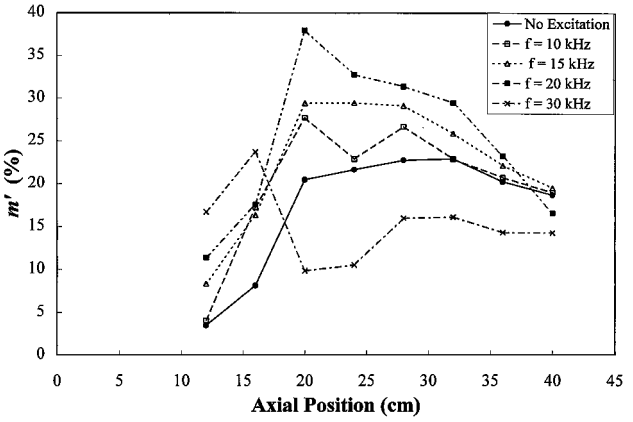

Fig. 12 Overall m' levels at various streamwise locations for each of five excitation conditions.

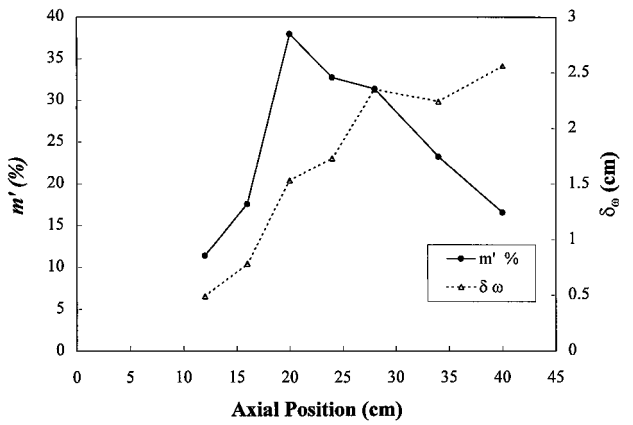

Fig. 13 Relationship between maximum m' levels and vorticity thickness levels for 20-kHz excitation case.

Brower[26] showed qualitatively similar results in which the peak fluctuation level moved further into the high-speed portion of the shear layer with increasing development downstream.

The maximum rms mass-velocity fluctuation levels m' at various streamwise locations are plotted in Fig. 12 for all five excitation cases, making use of the 20% position already described. The level of uncertainty for these measurements is estimated to be 10% (based on an axial probe location midway down the test section). The primary source of uncertainty is the accuracy of the fluctuating modal decomposition following the local linearization method first developed by Kovasznay.[27] Secondary uncertainty sources are associated with the probe positioning, ±0.5 mm and assuming the location of the maximum m' level a priori. Each case exhibits an increasing m' level through transition, but eventually these levels decrease. The m' levels for the excitation cases drop off further upstream and more drastically than does the m' level for the unexcited case. Zaman and Hussain[28] reported a similar behavior in the premature decay of centerline velocity fluctuations for an excited jet and explained the decrease based on coherent structure interactions leading to negative turbulence production. The hot-wire fluctuation measurement results are similar to the mean flow results of Fig. 6 in that the 20-kHz excitation case ($Sr = 1.63$) appears to be the dominant case. In general, the higher frequency excitations initially have rapid growing m' levels but then decrease almost as rapidly. The lower frequency excitation cases of 15 and 10 kHz and the unexcited case initially show less dramatic m' growth, but the growth is sustained over the length of the measurement region, as expected from linear stability theory. These results suggest, as do the mean flowfield data, that a more effective and sustained growth of the shear layer might be achieved by using higher excitation frequencies initially and gradually decreasing the excitation frequency as the shear-layer thickens. In theory, the wavy-wall wavelengths would have to be adjusted as well, to maintain a resonant interaction. Although such a variation in the excitation frequency could be achieved by a broader excitation spectrum and the wavy-wall wavelengths could be varied with downstream distance, such additional complexities are not practical and, thus, were not investigated.

Figure 13 finalizes the results by addressing the relationship between m' levels and vorticity thickness. The mean flowfield results of Fig. 6 are plotted simultaneously with the mass-velocity fluctuations, all for the 20-kHz excitation case. Figure 13 shows that m' changes tend to precede the vorticity thickness changes by a few shear-layer thicknesses in the upstream region of the plot. This is expected because the vorticity thickness is a mean flow measurement that depends on fluctuations for increased growth. Notice, however, that further downstream the m' level decreases drastically while the vorticity thickness continues to increase, although the rate of growth is decreasing. As already mentioned, the coherent structural motion interactions explained by Zaman and Hussain[28] are most likely responsible for this phenomenon.

Conclusions

The Mach-wave resonant interaction technique for shear-layer growth rate enhancement was examined experimentally with both mean and fluctuating measurements and glow excitation inputs. The wavy-wall condition with 20 kHz ($Sr = 1.63$) excitation exhibited the highest local shear-layer thickness growth rates, approximately 50% higher than the previous results for a smooth-wall, unexcited shear layer. Although this level of increase is not as high as anticipated based on numerical results, which predict increases of approximately 150%, it still indicates the potential for enhanced growth rates using the wavy-wall technique.

The numerical results are difficult to verify, but some indication of success is noted in the proximity between the numerical prediction of the most enhanced growth from resonant interaction occurring at just over 15 kHz ($Sr = 1.24$) compared to the predominant experimental result at 20 kHz ($Sr = 1.63$), especially when considering the numerical result corresponds to only one downstream location. The mass-velocity fluctuation measurements also demonstrated the 20-kHz component of excitation to be the most promising. Nonetheless, decreasing growth rates and fluctuation levels with increasing distance downstream suggest that the increasing shear-layer thicknesses (and associated length scales) eventually render the Mach-wave resonant interaction technique ineffective. In addition, the wall boundary layers can adversely affect shear-layer growth.

Informative schlieren visualizations of large-scale structures under various excitation conditions helped with the characterization of the flow physics within a wavy-wall environment. The tradeoff between growth rate and total pressure loss seems to indicate that wavy-wall disturbances are worth the enhancement they provide, but the measures of merit are not well defined. Finally, changes in mass-velocity fluctuations have been seen to precede changes in vorticity thickness in a comparable manner, at least in the upstream portion of the shear layer.

Acknowledgments

This research project has been partially supported by the Pennsylvania Space Grant Consortium. Additional support from a NASA Graduate Student Researchers' Program Fellowship monitored by J. M. Seiner and T. D. Norum is appreciated. The previous sponsorship of the Office of Naval Research (S. G. Lekoudis) and the Air Force Office of Scientific Research (J. M. Tishkoff) is also acknowledged. The assistance and discussion provided by P. J. Morris is also very much appreciated.

References

[1]Brown, G. L., and Roshko, A., "On Density Effects and Large Scale Structure in Turbulent Mixing Layers," *Journal of Fluid Mechanics*, Vol. 64, Pt. 4, 1974, pp. 775–816.

[2]Winant, C. D., and Browand, F. K., "Vortex Pairing: The Mechanism for Turbulent Mixing Layer Growth at Moderate Reynolds Number," *Journal of Fluid Mechanics*, Vol. 63, Pt. 2, 1974, pp. 237–255.

[3]Roshko, A., "Structure of Turbulent Shear Flows: A New Look," *AIAA Journal*, Vol. 10, No. 10, 1976, pp. 1349–1357.

[4]Bernal, L. P., and Roshko, A., "Streamwise Vortex Structure in Plane Mixing Layers," *Journal of Fluid Mechanics*, Vol. 170, 1986, pp. 499–525.

[5]Bell, J., and Mehta, R., "Three-Dimensional Structure of a Plane Mixing Layer," AIAA Paper 89-0124, Jan. 1989.

[6]Huang, L.-S., and Ho, C.-H., "Small-Scale Transition in a Plane Mixing Layer," *Journal of Fluid Mechanics*, Vol. 210, 1990, pp. 475–500.

[7]Birch, S. F., and Eggers, J. M., "A Critical Review of the Experimental Data for Developed Turbulent Free Shear Layers," NASA SP-321, 1973.

[8]Bogdanoff, D. W., "Compressibility Effects in Turbulent Shear Layers," *AIAA Journal*, Vol. 21, No. 6, 1983, pp. 926, 927.

[9]Papamoschou, D., and Roshko, A., "The Compressible Turbulent Shear Layer: An Experimental Study," *Journal of Fluid Mechanics*, Vol. 197, 1988, pp. 453–477.

[10]Oster, D., and Wygnanski, I., "The Forced Mixing Layer Between Parallel Streams," *Journal of Fluid Mechanics*, Vol. 123, 1982, pp. 91–130.

[11]Martens, S., Kinzie, K. W., and McLaughlin, D. K., "Measurements of Kelvin–Helmholtz Instabilities in a Supersonic Shear Layer," *AIAA Journal*, Vol. 32, No. 8, 1994, pp. 1633–1639.

[12]Papamoschou, D., "Structure of the Compressible Turbulent Shear Layer," AIAA Paper 89-0126, Jan. 1989.

[13]Fernando, E. M., and Menon, S., "Mixing Enhancement in Compressible Mixing Layers—An Experimental Study," AIAA Paper 91-1721, June 1991.

[14]Tam, K. W., and Hu, F. Q., "The Instability and Acoustic Wave Modes of Supersonic Mixing Layers Inside a Rectangular Channel," *Journal of Fluid Mechanics*, Vol. 203, 1989, pp. 51–76.

[15]Tam, K. W., and Hu, F. Q., "Resonant Instability of Ducted Free Supersonic Mixing Layers Induced by Periodic Mach Waves," *Journal of Fluid Mechanics*, Vol. 229, 1991, pp. 65–85.

[16]Gilreath, H. E., Sullins, G. A., and Raul, R., "Enhanced Fuel-Air Mixing in Hypersonic Engines," *Proceedings of the 11th International Symposium on Air Breathing Engines*, Vol. 2, AIAA, Washington, DC, 1993, pp. 1174–1181.

[17]Lee, L.-S, "Mixing Enhancement in Supersonic Compressible Shear Layers," Ph.D. Dissertation, Dept. of Aerospace Engineering, Pennsylvania State Univ., University Park, PA, May 1996.

[18]Martens, S., and McLaughlin, D. K., "Mixing Enhancement Using Mach Wave Interaction in a Confined Supersonic Shear Layer," AIAA Paper 95-2177, June 1995.

[19]Doty, M. J., "An Experimental Investigation of Mach Wave Interactions in a Compressible Mixing Layer," M.S. Thesis, Dept. of Aerospace Engineering, Pennsylvania State Univ., University Park, PA, Dec. 1998.

[20]Martens, S., "An Experimental Study of Compressible Mixing Layers," Ph.D. Dissertation, Dept. of Aerospace Engineering, Pennsylvania State Univ., University Park, PA, Aug. 1995.

[21]Gathmann, R. J., Si-Ameur, M., and Mathey, F., "Numerical Simulations of Three-Dimensional Natural Transition in the Compressible Confined Shear Layer," *Physics of Fluids*, Vol. 5, No. 11, 1993, pp. 2946–2968.

[22]Gustafson, M. D., Gilreath, H. E., and Sullins, G. A., "The Effects of Periodic Wall Boundary Conditions on a Confined Shear Layer Formed Between Supersonic Streams," *Proceedings of the 12th International Symposium on Air Breathing Engines*, Vol. 1, AIAA, Washington, DC, 1995, pp. 553–563.

[23]Browand, F. K., and Troutt, T. R., "The Turbulent Mixing Layer: Geometry of Large Scale Vortices," *Journal of Fluid Mechanics*, Vol. 158, 1985, pp. 489–509.

[24]Goebel, S. G., and Dutton, J. C., "Experimental Study of Compressible Turbulent Mixing Layers," *AIAA Journal*, Vol. 29, No. 4, 1991, pp. 538–546.

[25]Clemens, N. T., and Mungal, M. G., "Large-Scale Structure and Entrainment in the Supersonic Mixing Layer," *Journal of Fluid Mechanics*, Vol. 284, 1995, pp. 171–216.

[26]Demetriades, A., and Brower, T. L., "Experimental Study of Transition in a Compressible Free Shear Layer," Air Force Office of Scientific Research, AFOSR TR 83-0144, Bolling AFB, Washington, DC, Dec. 1982.

[27]Kovasznay, L. S. G., "The Hot-Wire Anemometer in Supersonic Flow," *Journal of the Aeronautical Sciences*, Vol. 17, No. 9, 1950, pp. 565–584.

[28]Zaman, K. B. M. Q., and Hussain, A. K. M. F., "Vortex Pairing in a Circular Jet Under Controlled Excitation. Part 2. Coherent Structure Dynamics," *Journal of Fluid Mechanics*, Vol. 101, Pt. 3, 1980, pp. 493–544.

M. Samimy
Associate Editor